Cluster Compounds

DOI: 10.1002/anie.200703069

$[Rh_7(PiPr_3)_6H_{18}][BAr^F{}_4]_2$: A Molecular Rh(111) Surface Decorated with 18 Hydrogen Atoms**

Simon K. Brayshaw, Jennifer C. Green, Ruth Edge, Eric J. L. McInnes, Paul R. Raithby,* John E. Warren, and Andrew S. Weller**

Many technologically important processes rely on the interaction of hydrogen with metal surfaces (for example, crude-oil hydrogenation, ammonia synthesis, electrooxidation of H_2 in a fuel cell).[1] However, directly observing hydrogen bound to a metal surface is not straightforward and requires the use of a limited set of high-vacuum techniques, such as electron-energy-loss spectroscopy (EELS) and scanning tunneling microscopy (STM).[2,3] Information that can be obtained from such experiments shows that on a Pt(111) surface atomic hydrogen is adsorbed to form a monolayer of hydrogen at 37 K, in which the H atoms are chemisorbed on threefold face-centered cubic sites and sit in the hollows between metal atoms.[2,3] Similar results were obtained for Rh(111) surfaces.[4]

Although many molecular metal clusters are known that form planar (or raftlike) structures that approximate M(111) surfaces, the metal sites are often saturated with carbonyl ligands—the consequence of a synthetic methodology that starts from carbonyl precursors.[5] Although interesting in their own right, such molecular materials are inappropriate models for metal surfaces in the absence of carbon monoxide.[6] We report herein novel cluster molecules that are not encumbered with carbonyl ligands, one of which has a planar Rh surface mimicking a M(111) monolayer, and—remarkably—18 hydride ligands associated with the metal atoms. The hydride ligands decorate the surface such that some of them reflect the experimentally (and theoretically) determined mode of attachment of hydrogen to an actual M(111) surface. As far as we are aware, this is the first time such an arrangement of hydrogen on a molecular metal cluster has been observed.

We recently reported the synthesis of the complex $[Rh_6(PiPr_3)_6H_{12}][BAr^F{}_4]_2$ [**1**$[BAr^F{}_4]_2$, $Ar^F = C_6H_3(CF_3)_2$; Eq (1)].[7]

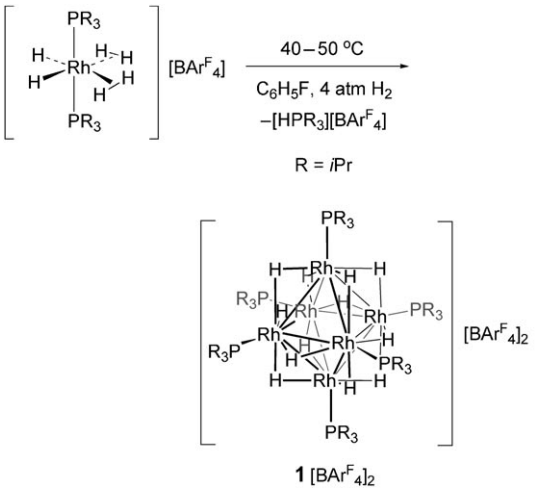

(1)

This molecule has an exceptional hydride content and can also store and release a further two equivalents of H_2.[7b,c] Evidence points to a mechanism for formation of **1**$[BAr^F{}_4]_2$ that involves heterolytic cleavage[8] of coordinated H_2 in precursor dihydrogen complexes $[Rh(PR_3)_2(H)_2(\eta^2\text{-}H_2)_2][BAr^F{}_4]$ (formed by hydrogenation of $[Rh(PR_3)_2(nbd)][BAr^F{}_4]$, nbd = norbornadiene), elimination of protonated phosphine $[HPR_3]^+$, and self-assembly of unsaturated mononuclear fragments.

We speculated that adding a source of "naked" rhodium to the reaction might result in the formation of larger clusters. Pleasingly, this is the case. Addition of $[Rh(nbd)_2][BAr^F{}_4]$ to a solution of $[Rh(PiPr_3)_2(nbd)][BAr^F{}_4]$ in fluorobenzene and addition of H_2 (ca. 4 atm) produces not only **1**$[BAr^F{}_4]_2$ and $[HPiPr_3][BAr^F{}_4]$, as observed previously,[7a] but also two new cluster materials that crystallize in low but reproducible overall yield (ca. 15%) from solution as an inseparable mixture [Eq (2)]. ESI mass spectrometry (ESI-MS), NMR and EPR spectroscopy, and X-ray crystallography identified these compounds as hepta- and octarhodium clusters $[Rh_7(PiPr_3)_6H_{18}][BAr^F{}_4]_2$ (**2**$[BAr^F{}_4]_2$) and $[Rh_8(PiPr_3)_6H_{16}][BAr^F{}_4]_2$ (**3**$[BAr^F{}_4]_2$), respectively. Changing the $[Rh(PiPr_3)_2(nbd)]$-

[*] Prof. J. C. Green
Department of Inorganic Chemistry
University of Oxford
Oxford, OX1 3QR (UK)
Fax: (+44) 1865-272-690
E-mail: jennifer.green@chem.ox.ac.uk
Dr. S. K. Brayshaw, Prof. P. R. Raithby, Dr. A. S. Weller
Department of Chemistry
University of Bath
Bath, BA2 7AY (UK)
Fax: (+44) 1225-386-231
E-mail: p.r.raithby@bath.ac.uk
a.s.weller@bath.ac.uk
Dr. R. Edge, Prof. E. J. L. McInnes
EPSRC Multi-frequency EPR Centre
School of Chemistry
University of Manchester
Manchester, M13 9PL (UK)
Dr. J. E. Warren
CCLRC Daresbury Laboratory
Daresbury, WA4 4AD (UK)

[**] We thank the EPSRC and the Royal Society for funding and Dr. Anneke Lubben for help acquiring the ESI-MS spectrum.
Supporting information for this article is available on the WWW under http://www.angewandte.org or from the author.

$$[Rh(P\mathit{i}Pr_3)_2(nbd)][BAr^F{}_4] + [Rh(nbd)_2][BAr^F{}_4] \xrightarrow[C_6H_5F,\ 4\ atm\ H_2]{40-50\ ^\circ C} \mathbf{2}\,[BAr^F{}_4]_2 + \mathbf{3}\,[BAr^F{}_4]_2 + [HP\mathit{i}Pr_3][BAr^F{}_4]\ \mathbf{1}\,[BAr^F{}_4]_2 + \text{other products, including} \quad (2)$$

$[BAr^F{}_4]$:$[Rh(nbd)_2][BAr^F{}_4]$ ratio or reaction time/temperature resulted in mixtures of these two products in varying ratios; compositionally pure material has not yet been produced. Thus, characterization was performed on a mixture, but, as we show, this allowed unequivocal identification of the products.

Figure 1 shows the solid-state structure of the metal cluster in $\mathbf{2}[BAr^F{}_4]_2$. In the crystal selected this cocrystallizes with octarhodium cluster $\mathbf{3}[BAr^F{}_4]_2$ so that 97% of the crystal is $\mathbf{2}[BAr^F{}_4]_2$ and only 3% is $\mathbf{3}[BAr^F{}_4]_2$. Different crystal batches gave different ratios of these two components. We restrict the analysis of $\mathbf{2}[BAr^F{}_4]_2$ to the crystalline material that has the lowest proportion of $\mathbf{3}[BAr^F{}_4]_2$, which allows the hydride ligands, of which there are 18 according to ESI-MS, to be satisfactorily modeled to the extent that they could be reliably located.

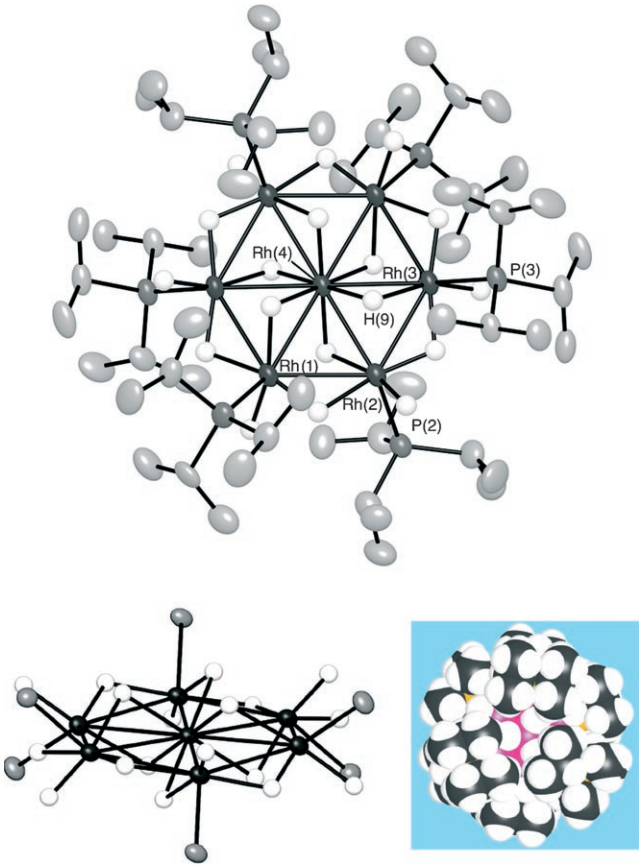

Figure 1. Molecular structure of $\mathbf{2}^{2+}$. Top: Thermal ellipsoids are shown at the 50% probability level. Only the component of 97% occupancy in the crystal is shown (see text). See the Supporting Information for full atom-labeling scheme. Hydrogen atoms (where shown) are included with an arbitrary radius. Selected distances: Rh(edge)–Rh(edge) 2.762(1)–2.772(1), Rh(edge)–Rh(center) 2.755(1)–2.770(1) Å. Bottom: Alternative views. The $[Rh_7P_6H_{18}]^{2+}$ core showing the arrangement of hydride and phosphine ligands (left) and space-filling diagram (right, van der Waals radii).

The core structure of $\mathbf{2}^{2+}$ is a planar wheel in which six {Rh(P*i*Pr$_3$)} fragments surround Rh(4), the central rhodium hub. The molecule is centrosymmetric with Rh(4) sitting on an inversion center. The Rh–Rh distances cover a small range between 2.755(1) and 2.770(1) Å (mean 2.767 Å) (compare $\mathbf{1}[BAr^F{}_4]_2$: 2.700(1)–2.733(1) Å, mean 2.720 Å), all reasonable for Rh–Rh bonding interactions (bulk Rh–Rh 2.70 Å). Six hydride ligands occupy terminal positions, and six bridge the Rh–Rh bonds around the rim. Six hydride ligands bridge the Rh–Rh spokes, alternately above and below the plane. Within the limitations inherent to X-ray crystallography, these hydride ligands are also tilted so that they lean towards the center of each Rh_3 triangle (for example, H(9)–Rh(2) 2.069(6) Å) and overall give the molecule approximate S_6 symmetry. Density functional calculations (see below) confirm this location, a further demonstration of the use of theoretical techniques to predict hydride locations on cluster species.[9]

The bulky P*i*Pr$_3$ ligands adopt a staggered, mutually *anti* arrangement around the rim of the molecule (Figure 1, bottom). That these ligands exert some steric strain on the central wheel is shown by each Rh atom on the ring being pulled slightly from the plane (0.10 Å) in the direction of the attached phosphine ligand. The cluster has an overall electron count of 91, and is thus expected to be paramagnetic.

The ^{1}H NMR spectrum of the sample with predominantly $\mathbf{2}[BAr^F{}_4]_2$ shows broad peaks for the alkyl phosphine groups, as well as a sharper one for the $[BAr^F{}_4]^-$ counterion. No significant hydride signals are observed at high field, as expected for a paramagnetic cluster species. A featureless $^{31}P\{^1H\}$ NMR spectrum is also observed. The EPR spectrum of $\mathbf{2}/\mathbf{3}[BAr^F{}_4]_2$ (frozen CD_2Cl_2 solution, see the Supporting Information) is dominated by an axial $S = 1/2$ spectrum with $g_{zz} = 2.522$ and $g_{xx} = g_{yy} = 2.054$, with no resolution of hyperfine coupling, together with a weaker signal due to a minor second species. The axial form of the spectrum is consistent with the approximate S_6 point symmetry of the cation, and both the unusually large g_{zz} value and lack of hyperfine resolution are consistent with the electronic structure as calculated by DFT methods (see below).

The closest structural analogues to $\mathbf{2}[BAr^F{}_4]_2$ are $Mn[\{Mn_7(CO)_{12}(thf)_6\}_2]$,[10] $[Au_6Ag(trip)_6]^+$ (trip = triisopropylphenyl,[11] $[Au_5Fe_2(CO)_8(dppm)_2]^+$ (dppm = bis(diphenylphosphino)methane),[12] $[M_5Fe_4(CO)_{16}]^{3-}$ (M = Cu, Ag),[13] and $[Os_6(\mu\text{-}Hg)(\mu\text{-}PPh_2)_2(CO)_{20}]$,[14] which have similar overall structures but no hydride ligands. The unusual structure of $\mathbf{2}^{2+}$ (and $\mathbf{3}^{2+}$) is no doubt accommodated by the bulky P*i*Pr$_3$ ligands that shield the metal core (Figure 1 bottom). Bulky alkyl phosphines are well known to stabilize unusual structures in clusters.[7,15]

The species that cocrystallizes with $\mathbf{2}[BAr^F{}_4]_2$ was identified by ESI-MS, NMR spectroscopy, and X-ray crystallography as the oblate cluster $[Rh_8(P\mathit{i}Pr_3)_6H_{16}][BAr^F{}_4]_2$ ($\mathbf{3}[BAr^F{}_4]_2$, Figure 2). An alternative crystal from a different reaction refined to a partial occupancy of $\mathbf{3}[BAr^F{}_4]_2$ of 45%, and it is this material on which the structural and spectroscopic analysis of $\mathbf{3}[BAr^F{}_4]_2$ is based. That $\mathbf{3}[BAr^F{}_4]_2$ cocrystallizes with $\mathbf{2}[BAr^F{}_4]_2$ (albeit in varying ratios) must be a

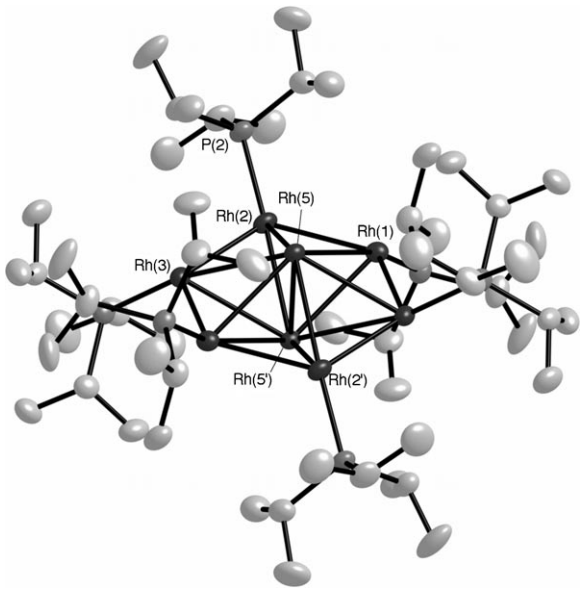

Figure 2. Molecular structure of $\mathbf{3}^{2+}$. Only the component of 45% occupancy in the crystal is shown (see text). Hydride atoms were not located. Rh(edge)–Rh(edge) 2.7231(2)–2.7396(3), Rh(edge)–Rh(center) 2.9635(5)–3.0676(5), Rh(center)–Rh(center) 2.553(1) Å.

consequence of the solid-state packing being dominated by the phosphine groups, which occupy a similar spatial arrangement for both. As for the cluster cation in $\mathbf{2}[BAr^F{}_4]_2$, $\mathbf{3}^{2+}$ adopts a centrosymmetric core structure. Hydride ligands were not all located experimentally, but ESI-MS showed there to be 16. The structure of $\mathbf{3}^{2+}$ is superficially similar to that of $\mathbf{2}^{2+}$, apart from the fact that the central Rh atom has been replaced by a Rh–Rh unit (d(Rh–Rh) = 2.553(1) Å). This distance is consistent with a Rh–Rh single bond (for example, $[Rh_2Cl_4(dppm)_2]$ 2.523(2) Å[16]). As far as we are aware, $\mathbf{3}[BAr^F{}_4]_2$ has no structural analogue.

Density functional calculations suggest a diamagnetic ground state for $\mathbf{3}^{2+}$, and solution NMR data confirm this. In the ^{1}H NMR spectrum, in addition to signals assigned to $[BAr^F{}_4]^-$ and the alkyl phosphine groups, signals attributable to 16 hydride ligands are observed between $\delta = -7.62$ and -17.97 ppm in the ratio 2:2:4(2+2):2:1:1:2:2, while in the ^{31}P{^{1}H} NMR spectrum three sharp signals are observed, all of which show coupling to ^{103}Rh, at $\delta = 82.8$, 81.1, and 76.3. Although not all the hydride ligands were located experimentallyby X-ray crystallography, their locations as suggested from DFT calculations (see below) are in excellent agreement with the observed patterns in the ^{1}H and ^{31}P{^{1}H} NMR spectra. Cooling to 240 K (CD_2Cl_2) resulted in broadening of all signals, due to low solubility at this temperature, but no significant changes in chemical shift, while warming a solution in $C_6H_4F_2$ resulted in the onset of decomposition at 313 K. Measurements of T_1 relaxation times suggest the ligands are hydride-like (240–260 ms).

Density functional calculations on $\mathbf{2}^{2+}$ (symmetry unconstrained, PH_3 replaces P*i*Pr$_3$, $S = 1/2$) replicate closely the X-ray structure, with the hydride ligands bridging the spokes and canted towards the Rh_3 triangle to give S_6 symmetry (Figure 3). The ring is rigorously planar, unlike the slight

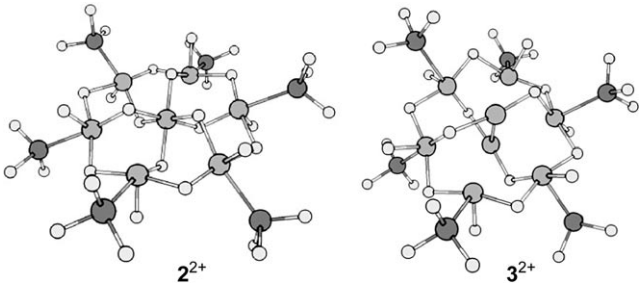

Figure 3. DFT calculated structures of $\mathbf{2}^{2+}$ and $\mathbf{3}^{2+}$ showing the geometry of the bridging hydride ligands (P*i*Pr$_3$ replaced by PH_3).

puckering observed experimentally, a consequence of the replacement of P*i*Pr$_3$ by PH_3 in the computational model. The Rh–Rh distances are calculated as 2.78 Å. The SOMO is a nonbonding orbital of A_u symmetry localized on the ring of six Rh atoms with no significant unpaired electron density on other atoms (Figure 4). Calculated spin densities are 0.16 for

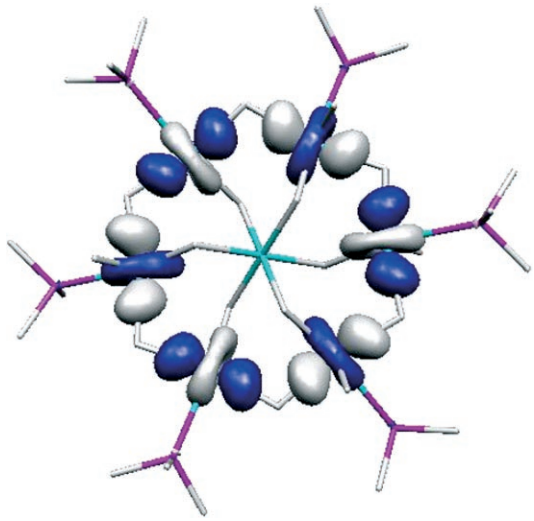

Figure 4. SOMO of $\mathbf{2}^{2+}$ (46 A_u level, cluster orbital localized on the peripheral Rh_6 ring).

the ring Rh and less than 0.01 for all other atoms. The SOMO–LUMO gap is relatively large (1.0 eV), while the highest lying filled MOs lie closer in energy starting 0.74 eV below the SOMO and are members of the ring Rh "t_{2g}" set. These latter metal-based orbitals are responsible for the large g_{zz} value in the EPR spectrum of **2**, as they include orbitals of A_u symmetry which mix with the SOMO under the combined action of spin–orbit coupling and an applied magnetic field parallel to the S_6 axis. Indeed, the DFT calculated g values ($g_{zz} = 2.561$, $g_{xx} = 2.054$, $g_{yy} = 2.053$) are in excellent agreement with the EPR experiment.

The nature of the SOMO is also consistent with the lack of metal hyperfine coupling in the EPR spectrum. Even if the SOMO is localized exclusively on the ring of six Rh ions, there is an unpaired electron density of 1/6 at each. Given the small nuclear magnetic moment of ^{103}Rh, and hence small electron–

nuclear dipolar coupling parameter,[17] we would expect a maximum dipolar hyperfine coupling of about 4 G to each Rh ion, which would easily be masked by the experimental line widths of about 30–40 G (calculated Rh ring A_{iso} is −0.11 Hz).

In modeling the structure of $\mathbf{3}^{2+}$ it was assumed that it shared with $\mathbf{2}^{2+}$ the common motif of an $[Rh_6(PR_3)_6H_{12}]$ ring. Given the total of sixteen hydride ligands and a relatively short axial Rh–Rh distance, a Rh_2H_4 unit was inserted into the ring in various starting orientations. Two low-energy structures were found: one with C_s symmetry (−185.14 eV) in which two of the H ligands are attached to the central Rh bridge spokes and two H ligands bridge faces, and one with C_2 symmetry (−185.09 eV) in which all four H ligands bridge spokes but are tilted towards the faces. Structures with $S > 0$ were found to be of higher energy in both cases. The patterns of the hydride and phosphine ligands in the C_2-symmetric structure (1:2:2:2:2:2:2:1 and 2:2:2, respectively) fit those observed in the ^1H and $^{31}P\{^1H\}$ NMR spectra, and thus we prefer this solution. The calculated Rh(edge)–Rh(edge) distances (2.62–2.65 Å) were shorter than found for $\mathbf{2}^{2+}$. The Rh(center)–Rh(center) distance (2.49 Å) and the Rh(center)–Rh(edge) distances (2.83–3.00 Å) were in reasonable agreement with the crystallographically determined values.

With regard to the bonding in the clusters, a $[Rh_6(PR_3)_6H_{12}]^{6+}$ ring provides seven low-lying empty orbitals for further bonding. In the case of $\mathbf{2}^{2+}$, six of these closely match the octahedrally disposed H atoms of a central $[RhH_6]^{3-}$ unit. The seventh holds the unpaired electron (Figure 4). In the case of $\mathbf{3}^{2+}$, the six orbitals form bridges to the four hydride ligands of an $[Rh_2H_4]$ unit and support the Rh–Rh bond. A more detailed description of the electronic structure will be given in a future publication.

Placing solid $\mathbf{2/3}[BAr^F_4]_2$ under dynamic vacuum (2×10^{-2} Torr, 16 h) does not remove any of the hydrogen, nor does placing under a hydrogen atmosphere (4 atm) result in addition of H_2 (by ESI-MS). This latter observation is in contrast to that for the clusters based on $\mathbf{1}[BAr^F_4]_2$, which, owing to two low-lying unoccupied orbitals,[7] can take up H_2 reversibly. The large SOMO–LUMO gap in $\mathbf{2}^{2+}$ (1.0 eV) is consistent with the lack of reactivity with H_2. Reduction with $[Cr(\eta^6\text{-}C_6H_6)_2]$ resulted in decomposition.

Cluster cation $\mathbf{2}^{2+}$ resembles a Rh(111) surface covered by hydrogen atoms, stabilized by peripheral bulky phosphine ligands. Although a handful of planar M_7 wheels have been described previously,[9–14] $\mathbf{2}[BAr^F_4]_2$ is the first example with hydride ligands, and its 18 hydride ligands make it one of the most hydride containing molecules known.[18] A closer inspection of the Rh_7 surface reveals that some of the hydride ligands occupy threefold hollows on the surface mimicking the experimentally observed situation of monolayer hydrogen coverage on a Pt(111) face-centered cubic surface (Figure 5).[2,3] This leads us to speculate that the reactions of $\mathbf{2}[BAr^F_4]_2$ with unsaturated compounds (alkenes, heteroalkenes) will lead to molecules that might mimic the reactivity of surfaces covered by hydrogen.

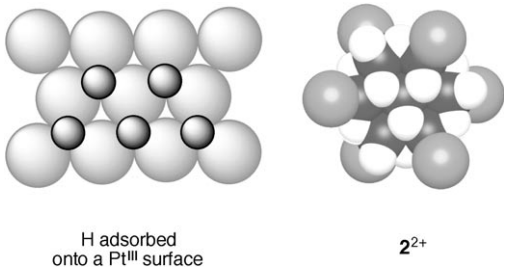

Figure 5. Comparison of the monolayer hydrogen coverage on a Pt(111) face-centered cubic surface with the position of the hydride ligands in $\mathbf{2}^{2+}$.

Experimental Section

In a typical experiment a solution of $[Rh(nbd)(P\mathit{i}Pr_3)_2][BAr^F_4]$ (200 mg, 0.145 mmol) and $[Rh(nbd)_2][BAr^F_4]$ (40 mg, 0.035 mmol) in fluorobenzene (20 mL) was placed under H_2 (4 atm), and the solution was heated at 40 °C for 6 days. The precipitate was collected to give dark red crystals (12.5 mg), which were found by ESI-MS to be an inseparable mixture of $\mathbf{2}[BAr^F_4]_2$ (5%) and $\mathbf{3}[BAr^F_4]_2$ (9%). Yields were determined from relative integrals of the $P\mathit{i}Pr_3$ ^1H NMR resonances of the mixture and are based on rhodium. The supernatant was found to contain a mixture of $\mathbf{1}[BAr^F_4]_2$, $[HP\mathit{i}Pr_3][BAr^F_4]$, and other unidentified products. ESI-MS (CH_2Cl_2) calcd for $[Rh_7P_6C_{54}H_{144}]^{2+}$: 849.6534, found: 849.6566; calcd for $[Rh_8P_6C_{54}H_{142}]^{2+}$: 900.0983, found: 900.0987.

NMR data for $\mathbf{2}[BAr^F_4]_2$: ^1H NMR (500.1 MHz, CD_2Cl_2): $\delta = 7.73$ (m, 16H; BAr^F_4), 7.57 (s, 8H; BAr^F_4), 1.33 ppm (brs, fwhm 110 Hz, 108H; CH_3).

NMR data for $\mathbf{2}[BAr^F_4]_2/\mathbf{3}[BAr^F_4]_2$ mixture: ^1H NMR (500.1 MHz, CD_2Cl_2): $\delta = 7.73$ (m, 16H; BAr^F_4), 7.57 (s, 8H; BAr^F_4), 2.39 (m, 6H; PCH), 2.01 (m, 12H; PCH), 1.10–1.50 (overlapping m, 108H; CH_3), −7.62 (brs, 2H; RhH), −11.35 (brs, 2H; RhH), −11.95 (br asymmetric, 2+2H; RhH), −13.06 (brm, 2H; RhH), −13.37 (brm, 1H; RhH), −16.12 (brm, 1H; RhH), −17.78 (s, 2H; RhH), −17.97 ppm (s, 2H; RhH). All hydride resonances show T_1 relaxation times of between 240 and 260 ms at 298 K. Attempts to determine T_1(min) were frustrated by the insolubility of the material at lower temperatures. $^{31}P\{^1H\}$ NMR: $\delta = 82.77$ (d, J(Rh,P) = 113 Hz, 2P), 81.07 (d, J(Rh,P) = 113 Hz, 2P), 76.34 ppm (d, J(Rh,P) = 146 Hz, 2P).

Density functional calculations were carried out using the Amsterdam Density Functional program suite ADF 2006.[19]

The X-band EPR spectrum of a frozen CD_2Cl_2 solution of **2/3** at 120 K was collected on a Bruker EMXmicro EPR spectrometer.

X-Ray crystallography: Crystal data for **2/3** (97/3%): $C_{124}H_{167}B_2F_{49}P_6Rh_{7.03}$, $M = 3562.80$, triclinic, space group $P\bar{1}$ (no. 2), $Z = 1$, $a = 14.5126(12)$, $b = 16.8575(14)$, $c = 17.2116(14)$ Å, $\alpha = 61.6980(1)$, $\beta = 87.970(1)$, $\gamma = 78.468(1)°$, $V = 3633.8(5)$ Å^3, $T = 150$ K, $\mu = 0.948$ mm^{-1}, $T_{min}/T_{max} = 0.96$, $2\theta_{max} = 56.0°$, 20478 reflections collected, 10297 unique [R(int) = 0.0419]. wR_2 0.1336 (all data). $R_1 = 0.0532$ ($I > 2\sigma(I)$). Crystal data for **2/3** (55/45%): $C_{124}H_{173}B_2F_{49}P_6Rh_{7.45}$, $M_r = 3568.73$, triclinic, space group $P\bar{1}$ (no. 2), $Z = 1$, $a = 14.5759(2)$, $b = 16.8176(2)$, $c = 17.2062(2)$ Å, $\alpha = 61.629(1)$, $\beta = 88.291(1)$, $\gamma = 79.019(1)°$, $V = 3633.73(8)$ Å^3, $T = 150$ K, $\mu = 0.998$ mm^{-1}, $T_{min}/T_{max} = 0.90$, $2\theta_{max} = 60.0°$, 69114 reflections collected, 21131 unique [R(int) = 0.0498]. wR_2 0.1054 (all data). $R_1 = 0.0417$ ($I > 2\sigma(I)$). CCDC-652792 (97/3) and CCDC-652793 (55/45) contain the supplementary crystallographic data for this paper. These

data can be obtained free of charge from The Cambridge Crystallographic Data Centre via www.ccdc.cam.ac.uk/data_request/cif.

Received: July 10, 2007
Published online: September 6, 2007

Keywords: cluster compounds · density functional calculations · hydride ligands · hydrogen · rhodium

[1] "Properties and Applications": Y. Fukai, *Hydrogen in Metals III* (Ed.: H. Wipf), Springer, Berlin, **1997**.
[2] H on Pt(111); experiment: a) T. E. Felter, E. C. Sowa, M. A. Van Hove, *Phys. Rev. B* **1989**, *40*, 891 – 899; b) T. Mitsui, M. K. Rose, E. Fomin, D. F. Ogletree, M. Salmeron, *Surf. Sci.* **2003**, *540*, 5 – 11; c) T. Mitsui, M. K. Rose, E. Fomin, D. F. Ogletree, M. Salmeron, *Nature* **2003**, *422*, 705 – 707; d) H. Conrad, G. Ertl, E. E. Latta, *Surf. Sci.* **1974**, *41*, 435 – 446.
[3] H on Pt(111); theory: J. Roques, C. Lacaze-Dufaure, C. Mijoule, *J. Chem. Theory Comput.* **2007**, *3*, 878 – 884, and references therein.
[4] H on Rh(111); experiment: H. Yanagita, H. Fujioka, T. Aruga, N. Takagi, M. Nishijima, *Surf. Sci.* **1999**, *441*, 507 – 514; theory: M. Mavrikakis, J. Rempel, J. Greeley, L. B. Hansen, J. K. Nørskov, *J. Chem. Phys.* **2002**, *117*, 6737 – 6744.
[5] R. D. Adams, B. Captain, W. Fu, M. B. Hall, J. Manson, M. D. Smith, C. E. Webster, *J. Am. Chem. Soc.* **2004**, *126*, 5253 – 5267.
[6] J. C. Green, E. A. Seddon, D. M. P. Mingos, *J. Chem. Soc. Chem. Commun.* **1979**, 94.
[7] a) S. K. Brayshaw, M. Ingleson, J. C. Green, P. R. Raithby, G. Kociok-Köhn, J. S. McIndoe, A. S. Weller, *J. Am. Chem. Soc.* **2006**, *128*, 6247; b) S. K. Brayshaw, J. S. McIndoe, F. Marken, P. R. Raithby, J. E. Warren, A. S. Weller, *J. Am. Chem. Soc.* **2007**, *129*, 1793; c) S. K. Brayshaw, J. C. Green, N. Hazari, J. S. McIndoe, F. M. Marken, P. R. Raithby, A. S. Weller, *Angew. Chem.* **2006**, *118*, 6151 – 6154; *Angew. Chem. Int. Ed.* **2006**, *45*, 6005 – 6008.
[8] a) G. J. Kubas, *Adv. Inorg. Chem.* **2004**, *56*, 127 – 178; b) M. J. Ingleson, S. K. Brayshaw, M. F. Mahon, G. D. Ruggiero, A. S. Weller, *Inorg. Chem.* **2005**, *44*, 3162 – 3171.
[9] a) S. K. Brayshaw, J. C. Green, N. Hazari, A. S. Weller, *Dalton Trans.* **2007**, 1781 – 1792; b) Y. Luo, J. Baldamus, O. Tardif, Z. M. Hou, *Organometallics* **2005**, *24*, 4362 – 4366.
[10] G. Kong, G. N. Harakas, B. R. Whittlesey, *J. Am. Chem. Soc.* **1995**, *117*, 3502 – 3509.
[11] E. Cerrada, M. Contel, A. D. Valencia, M. Laguna, T. Gelbrich, M. B. Hursthouse, *Angew. Chem.* **2000**, *112*, 2443 – 2446; *Angew. Chem. Int. Ed.* **2000**, *39*, 2353 – 2355.
[12] V. G. Albano, M. C. Iapalucci, G. Longoni, L. Manzi, M. Monari, *Organometallics* **1997**, *16*, 497 – 499.
[13] a) G. Doyle, K. A. Eriksen, D. Van Engent, *J. Am. Chem. Soc.* **1986**, *108*, 445 – 451; b) V. G. Albano, F. Azzaroni, M. C. Iapalucci, G. Longoni, M. Monari, S. Mulley, D. M. Proserpio, A. Sironi, *Inorg. Chem.* **1994**, *33*, 5320 – 5328.
[14] H. Egold, M. Schraa, U. Flörke, J. Partyka, *Organometallics* **2002**, *21*, 1925 – 1932.
[15] R. D. Adams, B. Captain, C. Beddie, M. B. Hall, *J. Am. Chem. Soc.* **2007**, *129*, 986 – 1000.
[16] F. A. Cotton, K. R. Dunbar, M. G. Verbruggen, *J. Am. Chem. Soc.* **1987**, *109*, 5498 – 5506.
[17] J. R. Morton, K. F. Preston, *J. Magn. Reson.* **1978**, *30*, 577.
[18] The raftlike complex $[Re_4Cu_2(PPhMe_2)_8H_{14}]$ also has a large number of hydride ligands, two of which sit over Re_2Cu hollow sites: B. R. Sutherland, D. M. Ho, J. C. Huffman, K. G. Caulton, *Angew. Chem.* **1987**, *99*, 147 – 149; *Angew. Chem. Int. Ed. Engl.* **1987**, *26*, 135 – 137.
[19] See the Supporting Information for full details and references.

